

Article

Remarkable Anti-Fouling Performance of TiO₂-Modified TFC Membranes with Mussel-Inspired Polydopamine Binding

Rui-Xin Zhang ¹, Leen Braeken ², Tian-Yin Liu ³, Patricia Luis ⁴, Xiao-Lin Wang ³ and Bart Van der Bruggen ^{1,*}

¹ Department of Chemical Engineering, KU Leuven, Celestijnenlaan 200f, Box 2424, 3001 Leuven, Belgium; ruixin.zh@gmail.com

² Department of Industrial Sciences, Lab4U, KH Limburg, Universitaire Campus, Gebouw B Bus 3, B-3590 Diepenbeek, Belgium; leen.braeken@kuleuven.be

³ State Key Laboratory of Chemical Engineering, Department of Chemical Engineering, Tsinghua University, 100084 Beijing, China; liu-ty10@mails.tsinghua.edu.cn (T.-Y.L.); xl-wang@tsinghua.edu.cn (X.-L.W.)

⁴ Materials & Process Engineering (iMMC-IMAP), Université catholique de Louvain, Place Sainte Barbe 2, 1348 Louvain-la-Neuve, Belgium; patricia.luis@uclouvain.be

* Correspondence: bart.vanderbruggen@kuleuven.be; Tel.: +32-1632-2340; Fax: +32-1632-2991

Academic Editor: Raed Abu-Reziq

Received: 2 December 2016; Accepted: 10 January 2017; Published: 13 January 2017

Abstract: It has been proven that a versatile bio-glue, polydopamine, can firmly bind TiO₂ (titanium dioxide) nanoparticles on thin film composite (TFC) membranes. In this work, the anti-fouling behaviour of this novel polydopamine-TiO₂-modified membrane is evaluated, based on the static bovine serum albumin (BSA) surface adhesion of the membranes and the relative flux decline. The results show that the anti-fouling performance of this new membrane is significantly improved in dark conditions when compared with the neat TFC membrane and the membranes only modified by polydopamine or TiO₂. When filtrating a 0.5 g·L⁻¹ BSA solution in dark conditions, the flux of the polydopamine-TiO₂-modified membrane remains constant, at 95% of its pure water flux after 30 min filtration for 8 h of the experiment. This indicates a significant increase in anti-fouling performance when compared to the 25% flux decline observed for the neat TFC membrane, and to the 15% flux decline of those only modified by polydopamine or TiO₂. This remarkable anti-fouling behaviour is attributed to an improved and uniform hydrophilicity, due to the presence of TiO₂ and to the regular nanosized papillae structure of the polydopamine-TiO₂ coating. Furthermore, since dopamine-modified TiO₂ has visible light-induced photocatalytic properties, the membrane's photocatalytic performance was also tested in light conditions. However an increase of flux and decrease of retention were observed after 24 h of continuous illumination, indicating that light may also affect the top layer of the membrane.

Keywords: anti-fouling; visible light photocatalysis; TiO₂ nanoparticles; dopamine; TFC membrane

1. Introduction

Through billions of years of evolution, creatures in nature have developed various remarkable functions for adapting themselves to the environment. Green plants, for instance, have developed photocatalysis, in order to utilize light energy to survive and thrive. *Ruellia devosiana* (a tropical plant) has developed a successful method of reducing fouling caused by organisms through the use of leaves with a superhydrophilic surface [1]. Inspired by these natural functions, advanced materials and processes have been developed to improve human life.

Mussels can attach themselves to almost any surface type such as rocks, pilings, aquatic plants, and floating debris, by the help of strong adhesive byssal (or byssus) threads. This adhesive property is attributed to a special chemical, dopamine [2]. Inspired by this function, dopamine was utilized as a versatile coating material, and it has been proved that it can self-polymerize on most surfaces of materials in base conditions [2]. Recently, it was demonstrated that dopamine polymerizes on nanoparticles [3–7], which allows nanoparticles to connect with bulk materials. This versatile connection may have a great potential for environmental applications, such as the immobilization of photocatalysts in photo-reactors, or the coating of photocatalysts on substrates to reduce fouling in air or water.

Among photocatalytic materials, titanium dioxide (TiO₂) is of interest for solar energy conversion and environmental applications, because of its superhydrophilic and photocatalytic properties. The combination of these two properties yields a material which has a good self-cleaning function on the surfaces of TiO₂. Similar to its function in *Ruellia devosiana*, the superhydrophilicity of TiO₂ is capable of letting water spread over the surfaces, forming an ultrathin water film which can significantly prevent pollutants from attaching. When illuminated by UV (ultraviolet) light, TiO₂ degrades organic pollutants through photocatalytic reactions, and keeps the surface clean. This self-cleaning function enables TiO₂ to be used in a variety of environmental applications [8]. In membrane filtration, the incorporation of TiO₂ nanoparticles into membrane matrixes or surfaces has received significant attention in recent years, and has been shown to improve the membranes' anti-fouling performance [9–20]. Several strategies for integrating TiO₂ into TFC membranes have been reported, including self-assembly [16,21–23], entrapment [24], and chemical binding [25,26]. For the entrapment method, the entirely enfolded TiO₂ nanoparticles do not yield the same performance of high hydrophilicity and good photochemical reactivity as the exposed bare nanoparticles, because of the shelter provided by the polymer matrix [24]. Furthermore, the higher concentration of TiO₂ nanoparticles inside the thin film may decrease the rejection of TFC membranes [24]. The chemical binding method can also improve the anti-fouling performance of the membranes, but this method can only be applied to certain kinds of TFC membranes, and it modifies the structure of the membrane surface [25]. When compared with these methods, the self-assembly method yields the best anti-fouling or self-cleaning performance of TiO₂, as the bare nanoparticles can be exposed to the environment. However, the main drawback of this method is the weak binding force between nanoparticles and membrane surfaces, which greatly limits the application of this modification method [27]. In order to overcome this limitation, mussel-inspired polydopamine has been used and has been reported to successfully bind TiO₂ nanoparticles on the membrane surface [28]. Additionally, this dopamine-modified TiO₂ is reported to enable adsorption in the visible light spectrum, and can be excited by visible light energies below 3.2 eV (~387.5 nm) [29]. These results potentially enable this polydopamine binding method to achieve a visible light-induced photocatalytic property, which is of possible interest to a variety of applications for achieving self-cleaning surfaces.

Although the robust binding force between the nanoparticles and membrane surfaces has been proved, the key issue, i.e., the anti-fouling performance of the membranes modified by TiO₂ using this novel polydopamine binding method, has not yet been reported. In this work, we will present a detailed study of the anti-fouling performance of membranes synthesised by this method, and compare it with reference membranes (i.e., the neat TFC membrane, the polydopamine-modified membrane, and the membrane modified by self-assembled TiO₂). Furthermore, the performance of the membrane modified by this method under visible light illumination is evaluated.

2. Theory

Hydraulic Resistance of Polydopamine and TiO₂-Modified Membranes

The hydraulic resistance of porous or non-porous membranes can be calculated using the following equation [10]:

$$R_i = \frac{\Delta P}{\eta J_w} = \frac{\Delta P \cdot t \cdot a}{\eta \cdot V} \quad (1)$$

where R_i is the hydraulic resistance of the membrane (m^{-1}), ΔP is the transmembrane pressure (Pa), η is the feed solution viscosity ($\text{Pa}\cdot\text{s}$), J_w is the pure water flux ($\text{m}^3\cdot\text{m}^{-2}\cdot\text{s}^{-1}$), and V (m^3) is the volume of water collected within a time period t (s) using a membrane of area a (m^2).

The modification procedures can influence the hydraulic resistance of the membranes. In order to evaluate this influence, an extension of Equation (1) is used, as follows:

$$J_{pDA} = \frac{\Delta P}{\eta(R_0 + R_{pDA})} \quad (2)$$

$$J_{\text{TiO}_2\text{-pDA}} = \frac{\Delta P}{\eta(R_0 + R_{\text{TiO}_2\text{-pDA}})} \quad (3)$$

And

$$J_{\text{TiO}_2\text{-self-assembly}} = \frac{\Delta P}{\eta(R_0 + R_{\text{TiO}_2\text{-self-assembly}})} \quad (4)$$

where J_{pDA} is the pure water flux of a polydopamine-modified membrane, $J_{\text{TiO}_2\text{-pDA}}$ is the pure water flux of a membrane modified by TiO_2 nanoparticles bound by polydopamine, and $J_{\text{TiO}_2\text{-self-assembly}}$ is the pure water flux of a membrane modified by TiO_2 nanoparticles bound by the self-assembly method. R_0 is the hydraulic resistance of the unmodified commercial TFC membrane. R_{pDA} , $R_{\text{TiO}_2\text{-pDA}}$, and $R_{\text{TiO}_2\text{-self-assembly}}$ are the hydraulic resistance of the polydopamine layer, the TiO_2 layer bound by polydopamine, and the TiO_2 layer bound by self-assembly method, respectively. The hydraulic resistance of each modification can be calculated by combining the equations above.

$$R_{pDA} = \frac{\Delta P}{\eta} \left(\frac{1}{J_{pDA}} - \frac{1}{J_0} \right) \quad (5)$$

$$R_{\text{TiO}_2\text{-pDA}} = \frac{\Delta P}{\eta} \left(\frac{1}{J_{\text{TiO}_2\text{-pDA}}} - \frac{1}{J_0} \right) \quad (6)$$

And

$$R_{\text{TiO}_2\text{-self-assembly}} = \frac{\Delta P}{\eta} \left(\frac{1}{J_{\text{TiO}_2\text{-self-assembly}}} - \frac{1}{J_0} \right) \quad (7)$$

where J_0 is the pure water flux of an unmodified commercial TFC membrane.

3. Materials and Methods

3.1. Materials

Desal51HL polyamide (Polypiperazineamide) thin film composite (TFC) membranes, manufactured by GE Osmonics (Minnetonka, MN, USA), were used in this study. Titanium (IV) oxide nanopowder (anatase, <25 nm, 99.7%) was provided by Sigma Aldrich (St. Louis, MO, USA). Dopamine hydrochloride (98.5%), bovine serum albumin (BSA, lyophilized powder, 96%), magnesium sulphate (MgSO_4), and sodium chloride (NaCl), were obtained from Sigma Aldrich (Schnelldorf, Germany). Tris (hydroxymethyl) aminomethane (99.8%) was supplied by Across Organics (Geel, Belgium).

3.2. Surface Modification of a Thin Film Composite (TFC) Membrane

Desal51HL polyamide TFC membranes were used for all surface modification procedures. Prior to each modification or test, the commercial TFC membranes were immersed in distilled water for 12 h [10]. Before using these membranes, they were all dried using compressed air for 5 min. This short-term drying procedure does not affect the filtration performance of the membranes [28]. In most cases, the modification procedures took place in a dead-end container (with a diameter of

100 mm), with a piece of dry Desal51HL membrane mounted on the bottom. If the modification was carried out in other cells with different diameters, the specific conditions will be specified. After this modification, the membranes were cut into a specific size for testing.

3.2.1. Polydopamine Modification

An aqueous dopamine solution was prepared by dissolving dopamine hydrochloride ($2 \text{ mg} \cdot \text{mL}^{-1}$) in Tris buffer solution (pH 8.5, 10 mM). A total of 40 mL of this fresh dopamine aqueous solution was poured into the dead-end container. The degree of dopamine polymerization can be observed from the change in color of the solution. The color becomes darker blue as the polymerization time increases. After 30 min of deposition, the membrane was rinsed using distilled water for 5 min in order to remove most of the residual unbound polydopamine.

3.2.2. Binding TiO_2 Nanoparticles on TFC Membranes by Using Polydopamine

A TiO_2 nanoparticles suspension of 0.05 *w/v* % was prepared by dispersing the commercial TiO_2 nanopowder in a Tris buffer solution (pH 8.5, 10 mM). After 3 h of agitation at 1000 rpm, the TiO_2 solution was further treated using ultrasound for 30 min in a water bath (20°C), in order to obtain a well-dispersed TiO_2 nanoparticles suspension.

Prior to the binding of the TiO_2 nanoparticles, the Desal51HL membranes were modified using polydopamine, as described in Section 3.2.1. After pouring out the residual polydopamine solution, 40 mL of TiO_2 nanoparticles suspension was added to the dead-end container for 1 h, and rinsed using distilled water for 5 min.

3.2.3. Binding TiO_2 Nanoparticles on TFC Membranes by Self-Assembly

The TiO_2 suspension of 0.05 *w/v* % was prepared as described above. The suspension (40 mL) was added to the dead-end container for 1 h, in order to allow the deposition of TiO_2 nanoparticles on the membrane surface. Following this, the membrane was rinsed with distilled water for 5 min.

3.3. Characterisation of the Membrane Surfaces

3.3.1. Scanning Electron Microscopy

The surface morphology of the membranes was characterized by scanning electron microscopy (SEM), using a Philips XL30 FEG SEM (Eindhoven, The Netherlands). The dry membrane was cut into small pieces and immersed in liquid nitrogen for around 1 min. The frozen fragments of the membrane were broken and taped onto a holder with carbon glue. The samples were sputtered with gold and vacuumed for 1 h before the measurement. The SEM measurements were taken under high vacuum conditions at 30 kV.

3.3.2. Contact Angle Measurement

A contact angle measuring system G10 (Krüss, Hamburg, Germany) was utilized to analyze the effect of the modification on the membrane hydrophilicity. A de-ionized water droplet of $2 \mu\text{L}$ was placed on a dry flat homogeneous membrane surface and the contact angle was measured after 5 s. Each measurement was taken at least 15 times and the average value was reported. The error was controlled below 3° .

3.3.3. UV-Visible Spectroscopy

A Shimadzu UV-1601 double beam spectrophotometer (SHIMADZU EUROPA GmbH, Duisburg, Germany) was used to analyze the amount of BSA in the solution. The absorption spectra of BSA were scanned in the range of 200–800 nm. The peak wavelength was located at 286 nm, which was used as the test wavelength.

3.3.4. Static BSA Surface Adhesion Measurement

The resistance to protein adsorption on the membrane surfaces was investigated by using the solution depletion method. In order to have a steady membrane surface, the membranes were rinsed for 90 min before each test. The membranes were placed in dead-end cells, and then incubated with 20 mL of BSA with a concentration of $0.5 \text{ g}\cdot\text{L}^{-1}$. The dead-end cells were sealed in order to prevent evaporation. The incubation time was 3 h. Before the measurement was taken, the cells were gently swirled to return loosely deposited BSA to the solution. The UV absorption percentage of this solution was tested, which indicated the amount of unabsorbed BSA. Each adsorption experiment was repeated three times [11].

3.4. Performance under Dark Conditions

3.4.1. Filtration Experiments under Dark Conditions

The studied membranes were characterised based on intrinsic water permeability and salt rejections (MgSO_4) using a transparent plastic dead-end cell (Figure 1, Amicon, Denver, MA, USA, model 8200), of which the active area was 28.7 cm^2 (a diameter of 63.5 mm). In order to avoid the influence of light on the intrinsic membrane performance, the dead-end cell was carefully covered by aluminum foil. To compare the filtration performance of the same membrane before and after the modification, the filtration experiments were performed in two steps: first of all, the neat Desal51HL membranes were evaluated and then, the performance of these TFC membranes after each modification (i.e., polydopamine modification, binding TiO_2 nanoparticles by polydopamine, and binding TiO_2 nanoparticles by self-assembly method), was tested.



Figure 1. Transparent plastic dead-end cell (Amicon, Denver, MA, USA, model 8200).

The vessel was filled with 200 mL of solution (pure water, MgSO_4 solution, or NaCl solution) and tested at ambient temperature. Since the maximum pressure limitation of the plastic dead-end cell was 5 bar, the transmembrane pressure was set at 4 bar. The permeate was collected when the membrane system reached a steady state. The pure water flux (J_w) was obtained by dividing the permeate volume by the membrane area and time. The pure water permeability (A) was calculated by dividing the pure water flux (J_w) by the transmembrane pressure (ΔP), $A = J_w / \Delta P$. After the pure water flux measurement had been taken, the rejections of MgSO_4 and NaCl were individually tested. The concentration of the feed solution was 2000 ppm in all cases. The pH of the salt solution was close to neutral (6.7–7.0). In order to reduce concentration polarization, the stirring speed was set at 700 rpm, in which condition the conductivity along the entire depth of solution was identical [28]. The salt rejections (R) were determined by measuring the conductivity of the permeate solution (c_p) and the concentrated solution (c_c), $R = 1 - c_p/c_c$.

After testing the filtration performance of the neat TFC membranes, the membranes were washed thoroughly with distilled water and dried under compressed air for 5 min. Following this, each modification procedure (i.e., polydopamine coating, binding TiO_2 by polydopamine, and binding

TiO₂ by self-assembly) was carried out inside the plastic dead-end modules, following the procedure described in Section 3.2. Since the diameter of the plastic dead-end cell was 63.5 cm, the volume of each solution used in the modification process was 14.35 mL. After further rinsing of the membranes for 30 min, the pure water permeability and the salt rejections of the modified membranes were tested again. Triplicates were performed for each modification procedure. Average values are reported.

3.4.2. Anti-Fouling Performance under Dark Conditions

In order to test the anti-fouling performance of the membranes in a relative long-term condition, the fouling filtration experiments were carried out in a cross-flow apparatus (Figure 2, Amafilter, Test Rig PSS1TZ), in which there was no light. The design of the experimental set-up is shown in Figure 2. The diameter of the membrane is 9 cm and the effective filtration area is 0.0059 m². As the system recycles the retentate and the permeate stream to the feed tank, the concentration of the feed solution was considered constant. A feed aqueous solution of 0.5 g·L⁻¹ BSA was filtrated for 8 h at 20 °C. Due to the minimum pressure limitation of this cross-flow filtration apparatus, the transmembrane pressure was set at 5 bar instead of 4 bar. The cross-flow velocity was 2.032 m·s⁻¹ (400 feet/min). In order to shorten the length of the whole procedure, the membranes were only compacted for 30 min before each test.

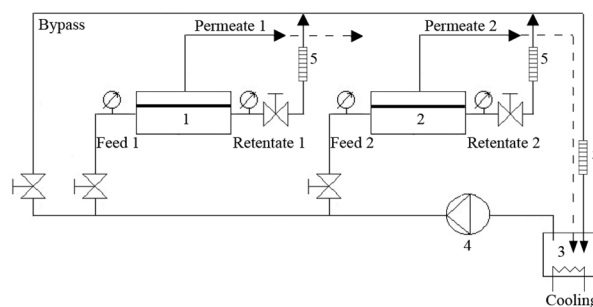


Figure 2. Schematic representation of the cross-flow nanofiltration unit (1, module 1; 2, module 2; 3, feed tank; 4, pump; 5, flow meter).

3.5. Performance under Light Conditions

3.5.1. Effect of Photocatalysis on Filtration Performance

In order to understand the effect of photocatalysis of bare TiO₂ and polydopamine-modified TiO₂ on the filtration performance, the membranes modified by TiO₂ using both binding methods were tested before and after visible light illumination. The experiments were performed in the transparent plastic dead-end cell. After each modification, the pure water permeability and salt rejections were tested. Following this, these membranes were illuminated using a 60-W bulb for 24 h, and the filtration performance was then tested again. The distance between the membrane surface and the bulb was 45 cm; at this distance, the heating of the light could be ignored, which was indicated by a thermometer located beside the dead-end cell.

3.5.2. Effect of Photocatalysis on Fouling Performance

Since it was impossible to provide light inside the cross-flow apparatus, the fouling filtration experiments in light conditions were performed in the transparent plastic dead-end cell. The illumination conditions are the same as described in Section 3.5.1. A total of 0.5 g·L⁻¹ of BSA solution was filtrated at 4 bar and ambient temperature. Because the testing period was 2 h, a slow stirring speed of 250 rpm was chosen to achieve a more obvious fouling condition, and the membranes were compressed for 90 min before each test. Triplicates were performed for each modification procedure. Average values are reported.

4. Results and Discussion

4.1. Characterisation of Membranes

4.1.1. Morphology of Unmodified and Modified Membranes

The surface morphology and roughness can influence liquid spreading and also further influence the fouling resistance of membranes. The surface morphology of both the unmodified and modified membranes is shown in Figure 3. It can be observed that the commercial TFC membrane has the smoothest surface. All of the modifications considered in this study can thus increase the roughness of the surfaces.

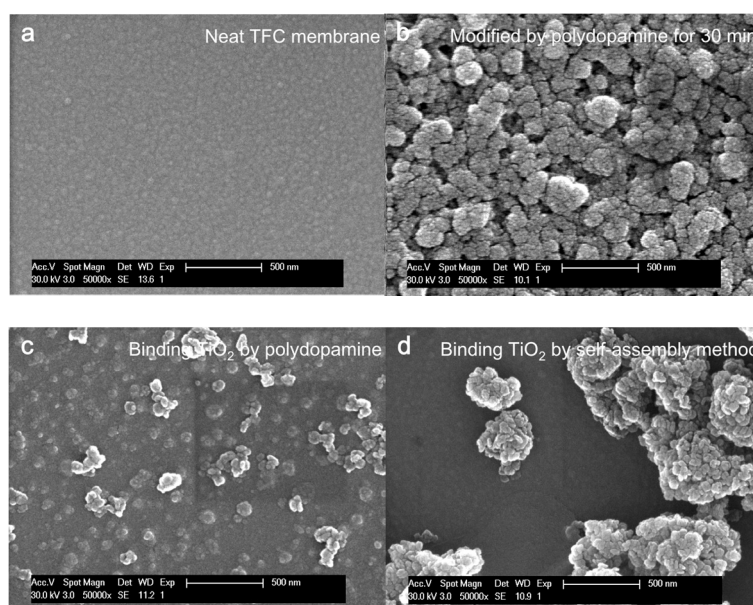


Figure 3. SEM (scanning electron microscopy) images displaying the unmodified and modified membranes: (a) unmodified commercial TFC (thin film composite) membranes; (b) TFC membranes modified by polydopamine for 30 min; (c) TFC membranes modified by TiO_2 nanoparticles (polydopamine method); (d) TFC membranes modified by TiO_2 nanoparticles (self-assembly method).

The mechanism of each modification has been reported [28,30–32]. The dopamine coating formed loose and relatively regular rough structures with nanoscale narrow valleys, as shown in Figure 3b. When the polydopamine layer made further contact with TiO_2 nanoparticles in suspension, nanoparticles filled all of the nanoscale valleys in the polydopamine surface, and the polydopamine had a chance to grow around the nanoparticles. Consequently, nanosized papillae surface structures are formed (Figure 3c), which is more uniform and flat than the structures shown in Figure 3b.

Compared with the surface morphology of the self-assembly binding method (Figure 3d), the polydopamine layer maintains a relatively uniform, identical, and complete coverage of TiO_2 nanoparticles on the membrane surfaces (Figure 3c). Generally, when the pDA-modified membrane makes contact with the TiO_2 suspension, the catechol/quinone groups on the polydopamine surface immediately attract the TiO_2 nanoparticles. Strong coordination bonds between the membranes and the nanoparticles keep TiO_2 nanoparticles in their initial position and prevent the nanoparticles from forming big clusters. Since the aqueous environment is basic, the residual dopamine monomers have a chance to polymerize between the nanoparticles and the membrane surface. As the immersion time increases, the oligomers gradually link with each other and grow around the nanoparticles, and the final structure is formed, as shown in Figure 3c. In the self-assembly method, when the membrane surface makes contact with the TiO_2 suspension, the coordination of Ti^{4+} to the electronegative group

(i.e., oxygen), or the hydrogen bond between carbonyl group and the surface hydroxyl group of TiO₂, keeps an uniform layer of TiO₂ nanoparticles on the surface in the initial stage. However, as the deposition time increases, the uniform TiO₂ nanoparticle layer tends to aggregate. Irregular, big TiO₂ clusters are formed, and the membrane surface is covered incompletely (Figure 3d).

4.1.2. Hydrophilicity of Surfaces

Self-cleaning surfaces are either superhydrophobic or superhydrophilic, such as *Nelumbo nucifera* (lotus leaves) and *Ruellia devosiana*. In water purification, hydrophilic surfaces are preferred, which can be achieved by changing both the surface roughness and the surface free energy [33,34]. In order to evaluate the hydrophilisation effect of the three modification methods, the water contact angle of the membrane surfaces was measured after 5 s (Table 1).

Table 1. Water contact angle for the unmodified and modified membranes.

Membranes	Neat	Neat + pDA	Neat + pDA + TiO ₂	Neat + TiO ₂
Contact angle	50.4 ± 2.3	59.3 ± 1.3	27.2 ± 2.9	24.5 ± 2.9

As shown in Table 1, the polydopamine coating slightly increases the contact angle of the membranes, which is similar to what was shown in the work of Yun [34]. The reason for this is probably related to a composite solid-liquid-air interface, formed between the water droplet and the polyamide surface. When the nanoscale narrow valleys of the polyamide layer make contact with water droplets, water may not penetrate into the surface cavities, which results in the formation of air pockets and leads to a composite interface [35]. As discussed by Cassie and Baxter [36], the contact angle increases for a hydrophilic surface with an increase of the fractional flat geometrical area of the liquid-air interface under the droplet. Furthermore, the nanoscale asperities can pin water droplets and thus prevent water from filling the valleys between the asperities [35]. Due to these reasons, the contact angle of the polydopamine-modified membrane is larger than the one of the unmodified membrane.

When the polydopamine layers further combine with TiO₂ nanoparticles, the surface free energy is greatly increased. This high surface free energy results in a significant reduction of the contact angle. For the self-assembly method, the TiO₂ clusters show the same behaviour as aforementioned.

4.1.3. Static BSA Adhesion Resistance

The BSA adhesion performance of each membrane is shown in Table 2. The UV absorption percentage indicates the amount of BSA in the solution after a 3 h incubation period. The larger value refers to less BSA adhesion, and also to higher BSA adhesion resistance. The membranes modified by TiO₂ using both binding methods adsorb less BSA in comparison to the neat TFC membrane and the membrane modified by polydopamine.

Table 2. UV (ultraviolet) absorption percentage of the BSA (bovine serum albumin) solution after a 3 h incubation period.

Solutions	Original BSA Solution	Neat	Neat + pDA	Neat + pDA + TiO ₂	Neat + TiO ₂
UV absorption percentage (%)	32.4 ± 0.7	19.3 ± 1.0	21.6 ± 1.2	29.7 ± 1.0	26.7 ± 1.4

This observation is in agreement with the fact that more hydrophilic surfaces adhere less protein under the same adsorption conditions [11,37]. However, the hydrophilicity does not seem to be the only factor that can influence the protein adhesion; the surface structures of the membranes and the functional groups also contribute to the protein adhesion ability. For example, the membrane modified by TiO₂ using polydopamine binding is less hydrophilic than the membrane modified by self-assembled TiO₂. This less hydrophilic surface does not lead to more protein adhesion. Instead,

it shows the best protein adhesion resistance. This is probably due to the relatively regular nanoscale papillae structure and the uniform hydrophilicity throughout the membrane surface. Although the surface roughness of the polydopamine-modified membrane is higher than the other membranes, the protein molecules cannot easily attach on the membrane surfaces. As suggested by Han et al. [38], the pore size of the polydopamine-modified surfaces is around 1.5 nm. The dimension of the prolate ellipsoid BSA is 14 nm for the major axis and 4 nm for the minor axis [39], which is significantly larger than the pore size of the polydopamine. Due to the larger size, BSA cannot settle into the pores of the polydopamine. In addition, the hydrolyzed surface functional groups (i.e., hydroxyl, quinone, and secondary amine groups), can repel the protein molecules, preventing them from attaching. These properties of the polydopamine layer lead to a better protein adhesion resistance [37].

4.2. Performance under Dark Conditions

4.2.1. Filtration Performance under Dark Conditions

Generally, any additional layer will change the hydraulic resistance of a membrane and further influence the filtration performance. The pure water permeability of the membranes before and after the modification is shown in Figure 4. The additional hydraulic resistance caused by each modification is summarized in Table 3. In order to assure that the differences in the performance for the modified membranes are caused by the modification, rather than by experimental errors, all of the tests are operated under exactly the same conditions.

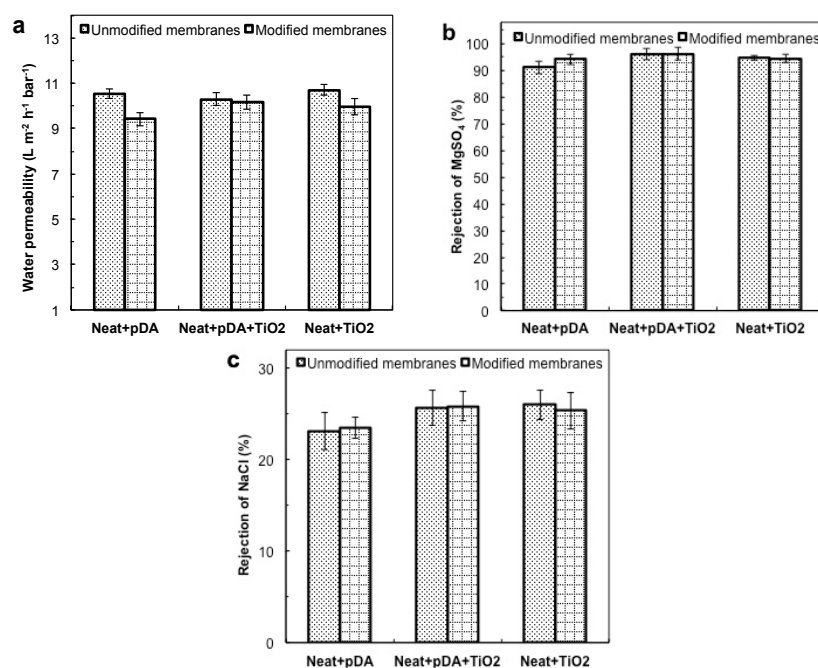


Figure 4. Filtration performance of the membranes before and after the modification. (a) Water permeability ($L \cdot m^{-2} \cdot h^{-1} \cdot bar^{-1}$); (b) Rejection of $MgSO_4$ (%); (c) Rejection of NaCl (5).

Table 3. Hydraulic resistance of the additional layers produced by different modification procedures.

Membranes	pDA Modified R_{pDA}	pDA + TiO ₂ Modified $R_{TiO_2_pDA}$	TiO ₂ Modified $R_{TiO_2_self-assembly}$
Hydraulic Resistance ($\times 10^{10} m^{-1}$)	40.28	4.47	25.27

As can be seen in Figure 4a, after each modification, the membrane modified by polydopamine displays the most flux reduction, when compared to the other modified membranes, indicating that

the polydopamine layer produces the highest hydraulic resistance (Table 3). This high hydraulic resistance is probably caused by a pore blockage of the support membrane and transport hindrance from polydopamine. When the dopamine contacts the membrane in the base aqueous condition, the size of polydopamine oligomers increases with increasing deposition time. The nanosized polydopamine oligomers presumably block the large pores of the membrane surfaces at the initial stage. As the deposition time increases, the thickness of the polydopamine layer also increases. Therefore, the hydraulic resistance of the final membrane increases and the pure water permeability is reduced by 10.5%. In the case of TiO₂ modification, less flux decline (6.99%) is observed. The performance of TiO₂ is a competition between hydrophilicity and a shelter effect. The large TiO₂ clusters formed by self-assembly can block the pores on the membrane surface. Moreover, the efficient surface area of these coagulated particles was limited. Therefore, the shelter effect was dominant, which results in a modest hydraulic resistance (Table 3). For the polydopamine binding method, the final composite layer (polydopamine together with TiO₂) yields a minimal flux decline (1.26%). When using this method, the nanoparticles are minimally coagulated because the dopamine monomers act as a surfactant at the initial stage. This good dispersion allows a relatively uniform layer of nanosized TiO₂ to bind on the membrane surfaces and provides a larger active surface area. This significantly larger surface area maximises the hydrophilic performance of TiO₂. In this case, the hydrophilicity of TiO₂ nanoparticles is dominant, and it greatly reduces the hydraulic resistance of the polydopamine layer (Table 3).

The rejection of MgSO₄ and NaCl is presented in Figure 4b,c. The polydopamine coating slightly increases the rejection of both salts. As previously mentioned, the nanosized polydopamine oligomers may block or grow in the defects or larger pores of the TFC membrane surfaces at the early stage, which possibly leads to a slight increase in the salt rejection. However, considering the rejection range and the standard deviation, there seems to be no significant difference in salt rejections for the membranes modified by TiO₂ using both binding methods.

4.2.2. Anti-Fouling Performance under Dark Conditions

In order to investigate the anti-fouling performance of the membranes in relatively long-term and dark conditions, each membrane was tested in the cross-flow apparatus. The fouling effect is quantified by the relative flux (J_i/J_0) and shown in Figure 5. It was found that, in the initial stage, the fluxes of the neat membrane and the membrane modified by polydopamine, decrease more rapidly than the others. This rapid flux decline is attributed to the relatively large contact angles. Following this, the flux of each membrane reaches its equilibrium. The membrane modified by TiO₂ using the polydopamine binding method reaches an equilibrium value of 95% after 30 min of filtration. The fluxes of the membranes modified by polydopamine and self-assembled TiO₂ stabilize at around 85% of the initial value after 2 h of filtration. After 8 h of filtration, the neat membrane retains around 75% of the initial flux. This fouling behavior is following the trend in the static BSA adhesion test (Section 4.1.3, Table 2): the membrane with good static BSA adhesion resistance has better anti-fouling filtration performance. The reasons for the fouling behavior are also consistent with the discussion in Section 4.1.3.

When comparing the initial anti-fouling performance of the membranes modified by TiO₂ with both self-assembly and polydopamine methods, it can be found that the robust binding of TiO₂, as shown in our previous work [28], is crucial for maintaining a constant and good anti-fouling performance. A large fraction of the self-assembled TiO₂ can be removed by the water flow in the first hour of filtration [40]. A lower quantity of TiO₂ results in lower hydrophilicity and worse protein adhesion resistance. Figure 5 shows that the unstable bound TiO₂ cannot retain the same performance when the filtration time increases, although the membrane modified by self-assembled TiO₂ has a good anti-fouling performance in the initial 30 min of filtration. When further increasing the filtration time, the quantity of TiO₂ gradually decreases [40], which leads to a reduction in hydrophilicity and the loss of protein adhesion resistance. On the contrary, the polydopamine binding method can successfully overcome this limitation, maintaining a constant and good anti-fouling performance.

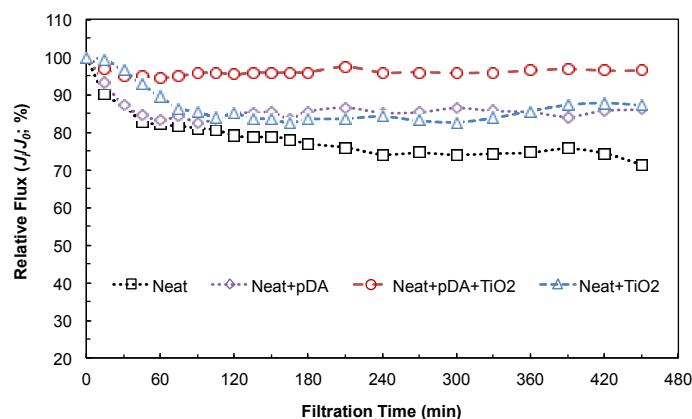


Figure 5. Relative flux of the unmodified (neat) and modified membranes as a function of time during the filtration of BSA (bovine serum albumin) ($0.5 \text{ g}\cdot\text{L}^{-1}$) in dark conditions.

4.3. Performance under Light Conditions

4.3.1. Effect of Photocatalysis on Filtration Performance

The membrane modified by TiO_2 using the polydopamine binding method has a remarkable anti-fouling performance in dark conditions—as described above. However, since TiO_2 modified by dopamine can be excited by visible light, the performance of this visible light-induced photocatalysis is evaluated here. The membrane modified by polydopamine- TiO_2 was tested before and after visible light illumination. The pure water flux and salt rejections are shown in Figure 6a. It was found that the flux was significantly higher (by 61.2%), and the salt rejections of MgSO_4 and NaCl decreased by 43.9% and by 11.1%, respectively, after 24 h of illumination. To make sure that these changes were caused by the polydopamine-modified TiO_2 , instead of the bare TiO_2 , the membrane modified by bare TiO_2 using the self-assembly method was tested as a reference. The filtration performance of this self-assembly method was not significantly different (<2%) either before or after the illumination (Figure 6b). When comparing the filtration performance of these two methods after illumination (Figure 6a,b), the results indicate that the functional top layers (polydopamine and/or polyamide) of the membrane modified by polydopamine- TiO_2 was probably degraded by the visible light-induced photocatalysis of the polydopamine-modified TiO_2 .

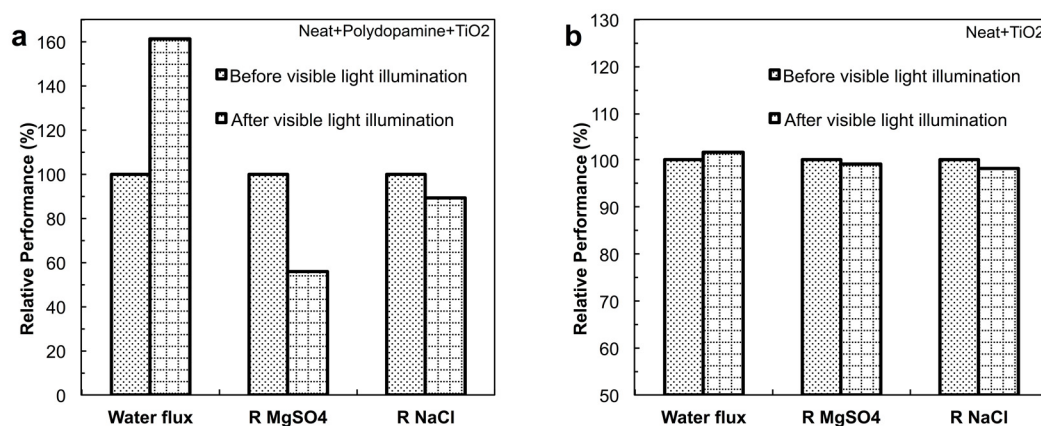


Figure 6. Filtration performance of the modified membranes before and after the visible light illumination for 24 h: (a) the membrane modified by TiO_2 using polydopamine binding method; (b) the membrane modified by TiO_2 using self-assembly method.

The mechanism of this visible light-induced photocatalytic degradation is as follows. Modification of TiO₂ nanoparticles using dopamine or polydopamine promotes spatial separation charges. Since holes localize on dopamine and electrons localize in the lattice of TiO₂, the recombination of charges is suppressed [29]. This dopamine (or polydopamine) modified TiO₂ enables adsorption in the visible light spectrum, and can be excited by visible light energies below 3.2 eV (~387.5 nm) [29]. In this spectrum range, bare TiO₂ cannot be excited, because the energy of these photons is not sufficient to excite electrons from the valence band to the conduction band of TiO₂. In this situation, the well-known redox chemical reactions generated by photoexcitation of bare TiO₂ cannot happen. For dopamine- (or polydopamine) modified TiO₂, the formation of reactive oxygen species can be produced by multiple redox chemistries under visible light illumination. Dimitrijevic et al. [29] reported that the spatial separation caused by the presence of dopamine does not affect the properties of photogenerated electrons. The reduction of oxygen molecules and formation of superoxide anions as precursors for some reactive oxygen species is not influenced. All of these reactive oxygen species produced by the visible light excitation of dopamine- (or polydopamine) modified TiO₂ results in the degradation of the membrane surface. This degradation suggests that the TiO₂-modified membranes using polydopamine should be stored in dark conditions in order to maintain the filtration performance. Alternatively, the membrane surface should be covered by a protective layer. If this polydopamine binding method is utilized under light conditions (e.g., in photo-reactors), antioxidizing reagents should be added inside and/or under the polydopamine layer.

4.3.2. Effect of Photocatalysis on Fouling Performance

In order to investigate the anti-fouling performance of the membrane modified by polydopamine-TiO₂ under light conditions, the membranes were tested in the transparent dead-end cell, and the results are shown in Figure 7.

After 90 min of compaction by stirring the pure water, the composition (i.e., TiO₂) of the membrane surfaces becomes stable. When these membranes make contact with the BSA solution, the fluxes drop immediately, and approach their equilibrium. The neat membrane, the polydopamine coated membrane, and the membrane modified by self-assembled TiO₂, retain around 85%, 88%, and 88% of their pure water fluxes, respectively, after 2 h of fouling experiment, and these membranes demonstrate similar flux trends to the ones in the dark conditions (Figures 5 and 7). This similar anti-fouling behaviour in the light and dark conditions indicates that the light has no significant influence on the anti-fouling performance of the aforementioned membranes.

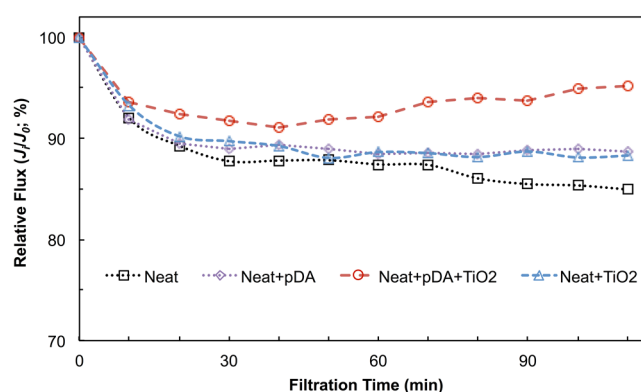


Figure 7. Relative flux of the unmodified (neat) and modified membranes as a function of time during the filtration of BSA (0.5 g·L⁻¹) in light conditions.

Unlike these membranes, the membrane modified by TiO₂ using polydopamine shows a different anti-fouling behaviour between the light and dark conditions. Other than reaching an equilibrium state in the dark conditions, the flux of the membrane modified by polydopamine-TiO₂ drops to 91%

of the pure water flux first, and then slowly increases to around 95%. Since it is difficult to track the dynamic changes in the structures of the membrane surfaces, it can be assumed that this slight increase of the flux in the light conditions is probably either caused by degradation of the top layers as discussed in Section 4.3.1, or caused by the removal of the BSA layer from the surfaces.

The holes on the surfaces of dopamine-modified TiO₂ are not capable of oxidizing water molecules to OH radicals, and the major part of the reactive oxygen species formed by visible light illumination in aqueous conditions, are superoxide anions [41]. As the illumination time increases, the superoxide anions accumulate on the membrane surface. These actions might have two consequences: (1) the superoxide anions degrade the top layer of the membrane; (2) these accumulated anions slowly increase the surface charge and the hydrophilicity of the membrane surface, which helps to loosen the attached BSA layer and also to avoid the BSA from attaching. The work suggests that the visible light illumination has an effect on the fouling performance of the membrane modified by this polydopamine-TiO₂. However, the real mechanisms still need to be further explored in the future.

5. Conclusions

In this study, a biomimetic glue, polydopamine, is used to firmly bind TiO₂ nanoparticles on the surface of a TFC membrane, and this polydopamine-TiO₂-modified membrane shows a remarkable anti-fouling performance (i.e., low static BSA surface adhesion, low additional membrane resistance, and less relative flux decline), when compared to the neat membrane and the membranes modified by polydopamine or TiO₂. When filtrating 0.5 g·L⁻¹ of BSA solution for 8 h in dark conditions, the flux of the membrane modified by polydopamine-TiO₂ stabilizes at around 95% of its pure water flux value after 30 min of filtration. The good anti-fouling performance of the polydopamine-TiO₂-modified membrane is attributed to: (1) the improved hydrophilicity; (2) the relatively uniform coverage of TiO₂ nanoparticles on the membrane surface; and (3) the special relatively regular nanosized papillae surface structures. In addition to the good anti-fouling performance, the polydopamine-TiO₂ modified membrane can also maintain a similar filtration performance to the initial neat membrane in dark conditions. However, for the membranes only modified by polydopamine or TiO₂, the fluxes all decrease because of the additional hydraulic resistance.

Since photocatalysis of polydopamine-modified TiO₂ nanoparticles can be induced by visible light, the effect of visible light photocatalysis on the filtration and performance was also investigated. However, the results show that the visible light photocatalysis of the polydopamine-modified TiO₂ can degrade the surface structures of the membranes. Due to these advantages and drawbacks, it is suggested that this polydopamine binding method should be applied in dark conditions, in order to achieve the best, long-term anti-fouling performance. If the function of photocatalysis is required, an anti-oxidizing reagent should be added to the polydopamine solution or to the membranes, which still needs to be systemically investigated.

Author Contributions: Rui-Xin Zhang, Leen Braeken and Bart Van der Bruggen conceived and designed the experiments; Rui-Xin Zhang performed the experiments; Rui-Xin Zhang, Leen Braeken and Patricia Luis analyzed the data; Rui-Xin Zhang wrote the paper; Rui-Xin Zhang, Leen Braeken, Tian-Yin Liu, Xiao-Lin Wang and Bart Van der Bruggen reviewed and revised the paper.

Conflicts of Interest: The authors declare no conflict of interest.

References

1. Koch, K.; Barthlott, W. Superhydrophobic and superhydrophilic plant surfaces: An inspiration for biomimetic materials. *Philos. Trans. R. Soc. A Math. Phys. Eng. Sci.* **2009**, *367*, 1487–1509. [[CrossRef](#)] [[PubMed](#)]
2. Lee, H.; Dellatore, S.M.; Miller, W.M.; Messersmith, P.B. Mussel-inspired surface chemistry for multifunctional coatings. *Science* **2007**, *318*, 426–430. [[CrossRef](#)] [[PubMed](#)]
3. Zhou, W.-H.; Lu, C.-H.; Guo, X.-C.; Chen, F.-R.; Yang, H.-H.; Wang, X.-R. Mussel-inspired molecularly imprinted polymer coating superparamagnetic nanoparticles for protein recognition. *J. Mater. Chem.* **2010**, *20*, 880–883. [[CrossRef](#)]

4. Peng, L.; Guo, R.; Lan, J.; Jiang, S.; Lin, S. Microwave-assisted Deposition of Silver Nanoparticles on Bamboo Pulp Fabric through Dopamine Functionalization. *Appl. Surf. Sci.* **2016**, *386*, 151–159. [[CrossRef](#)]
5. Yuan, Z.; Zhao, Y.; Yang, W.; Hu, Y.; Cai, K.; Liu, P.; Ding, H. Fabrication of antibacterial surface via UV-inducing dopamine polymerization combined with co-deposition Ag nanoparticles. *Mater. Lett.* **2016**, *183*, 85–89. [[CrossRef](#)]
6. Zhuang, M.-Y.; Zhou, Q.-L.; Wang, X.-Y.; Zhang, J.-X.; Xue, L.; Wang, R.; Zhang, J.-X.; Zhang, Y.-W. Immobilization of Lipase Onto Dopamine Functionalized Magnetic Nanoparticles. *Nanosci. Nanotechnol. Lett.* **2016**, *8*, 251–254. [[CrossRef](#)]
7. He, W.; Ding, Y.; Zhang, W.; Ji, L.; Zhang, X.; Yang, F. A highly sensitive sensor for simultaneous determination of ascorbic acid, dopamine and uric acid based on ultra-small Ni nanoparticles. *J. Electroanal. Chem.* **2016**, *775*, 205–211. [[CrossRef](#)]
8. Liu, K.; Jiang, L. Bio-inspired self-cleaning surfaces. *Annu. Rev. Mater. Res.* **2012**, *42*, 231–263. [[CrossRef](#)]
9. Kasemset, S.; Lee, A.; Miller, D.J.; Freeman, B.D.; Sharma, M.M. Effect of polydopamine deposition conditions on fouling resistance, physical properties, and permeation properties of reverse osmosis membranes in oil/water separation. *J. Membr. Sci.* **2012**, *425–426*, 208–216. [[CrossRef](#)]
10. McCloskey, B.D.; Park, H.B.; Ju, H.; Rowe, B.W.; Miller, D.J.; Chun, B.J.; Kin, K.; Freeman, B.D. Influence of polydopamine deposition conditions on pure water flux and foulant adhesion resistance of reverse osmosis, ultrafiltration, and microfiltration membranes. *Polymer* **2010**, *51*, 3472–3485. [[CrossRef](#)]
11. Azari, S.; Zou, L. Using zwitterionic amino acid L-DOPA to modify the surface of thin film composite polyamide reverse osmosis membranes to increase their fouling resistance. *J. Membr. Sci.* **2012**, *401*, 68–75. [[CrossRef](#)]
12. Miller, D.J.; Araújo, P.A.; Correia, P.; Ramsey, M.M.; Kruithof, J.C.; van Loosdrecht, M.; Freeman, B.D.; Paul, D.R.; Whiteley, M.; Vrouwenvelder, J.S. Short-term adhesion and long-term biofouling testing of polydopamine and poly (ethylene glycol) surface modifications of membranes and feed spacers for biofouling control. *Water Res.* **2012**, *46*, 3737–3753. [[CrossRef](#)] [[PubMed](#)]
13. McCloskey, B.D.; Park, H.B.; Ju, H.; Rowe, B.W.; Miller, D.J.; Freeman, B.D. A bioinspired fouling-resistant surface modification for water purification membranes. *J. Membr. Sci.* **2012**, *413–414*, 82–90. [[CrossRef](#)]
14. Pan, F.; Jia, H.; Qiao, S.; Jiang, Z.; Wang, J.; Wang, B.; Zhong, Y. Bioinspired fabrication of high performance composite membranes with ultrathin defect-free skin layer. *J. Membr. Sci.* **2009**, *341*, 279–285. [[CrossRef](#)]
15. Cheng, C.; Li, S.; Zhao, W.; Wei, Q.; Nie, S.; Sun, S.; Zhao, C. The hydrodynamic permeability and surface property of polyethersulfone ultrafiltration membranes with mussel-inspired polydopamine coatings. *J. Membr. Sci.* **2012**, *417–418*, 228–236. [[CrossRef](#)]
16. Fischer, K.; Grimm, M.; Meyers, J.; Dietrich, C.; Gläser, R.; Schulze, A. Photoactive microfiltration membranes via directed synthesis of TiO₂ nanoparticles on the polymer surface for removal of drugs from water. *J. Membr. Sci.* **2015**, *478*, 49–57. [[CrossRef](#)]
17. Ngo, T.H.A.; Nguyen, D.T.; Do, K.D.; Nguyen, T.T.M.; Mori, S.; Tran, D.T. Surface modification of polyamide thin film composite membrane by coating of titanium dioxide nanoparticles. *J. Sci. Adv. Mater. Devices* **2016**, *1*, 468–475. [[CrossRef](#)]
18. Alvarado, C.; Farris, K.; Kilduff, J. Membrane Fouling, Modelling and Recent Developments for Mitigation. *Emerg. Membr. Technol. Sustain. Water Treat.* **2016**, 433–462. [[CrossRef](#)]
19. Lu, D.; Zhang, T.; Gutierrez, L.; Ma, J.; Croue, J.-P. Influence of surface properties of filtration-layer metal oxide on ceramic membrane fouling during ultrafiltration of oil/water emulsion. *Environ. Sci. Technol.* **2016**, *50*, 4668–4674. [[CrossRef](#)] [[PubMed](#)]
20. Zhang, W.; Ding, L.; Luo, J.; Jaffrin, M.Y.; Tang, B. Membrane fouling in photocatalytic membrane reactors (PMRs) for water and wastewater treatment: A critical review. *Chem. Eng. J.* **2016**, *302*, 446–458. [[CrossRef](#)]
21. Kim, S.H.; Kwak, S.-Y.; Sohn, B.-H.; Park, T.H. Design of TiO₂ nanoparticle self-assembled aromatic polyamide thin-film-composite (TFC) membrane as an approach to solve biofouling problem. *J. Membr. Sci.* **2003**, *211*, 157–165. [[CrossRef](#)]
22. Madaeni, S.; Ghaemi, N. Characterization of self-cleaning RO membranes coated with TiO₂ particles under UV irradiation. *J. Membr. Sci.* **2007**, *303*, 221–233. [[CrossRef](#)]
23. Kwak, S.-Y.; Kim, S.H.; Kim, S.S. Hybrid organic/inorganic reverse osmosis (RO) membrane for bactericidal anti-fouling. 1. Preparation and characterization of TiO₂ nanoparticle self-assembled aromatic polyamide thin-film-composite (TFC) membrane. *Environ. Sci. Technol.* **2001**, *35*, 2388–2394. [[CrossRef](#)] [[PubMed](#)]

24. Lee, H.S.; Im, S.J.; Kim, J.H.; Kim, H.J.; Kim, J.P.; Min, B.R. Polyamide thin-film nanofiltration membranes containing TiO₂ nanoparticles. *Desalination* **2008**, *219*, 48–56. [[CrossRef](#)]
25. Mansourpanah, Y.; Madaeni, S.; Rahimpour, A.; Farhadian, A.; Taheri, A. Formation of appropriate sites on nanofiltration membrane surface for binding TiO₂ photo-catalyst: Performance, characterization and fouling-resistant capability. *J. Membr. Sci.* **2009**, *330*, 297–306. [[CrossRef](#)]
26. Mo, J.; Son, S.H.; Jegal, J.; Kim, J.; Lee, Y.H. Preparation and characterization of polyamide nanofiltration composite membranes with TiO₂ layers chemically connected to the membrane surface. *J. Appl. Polym. Sci.* **2007**, *105*, 1267–1274. [[CrossRef](#)]
27. Rajh, T.; Dimitrijevic, N.M.; Rozhkova, E.A. Titanium Dioxide Nanoparticles in Advanced Imaging and Nanotherapeutics. In *Biomedical Nanotechnology*; Springer: Berlin, Germany, 2011; pp. 63–75.
28. Zhang, R.-X.; Braeken, L.; Luis, P.; Wang, X.-L.; Van der Bruggen, B. Novel binding procedure of TiO₂ nanoparticles to thin film composite membranes via self-polymerized polydopamine. *J. Membr. Sci.* **2013**, *437*, 179–188. [[CrossRef](#)]
29. Dimitrijevic, N.M.; Rozhkova, E.; Rajh, T. Dynamics of localized charges in dopamine-modified TiO₂ and their effect on the formation of reactive oxygen species. *J. Am. Chem. Soc.* **2009**, *131*, 2893–2899. [[CrossRef](#)] [[PubMed](#)]
30. Liu, L.; Shao, B.; Yang, F. Polydopamine coating–surface modification of polyester filter and fouling reduction. *Sep. Purif. Technol.* **2013**, *118*, 226–233. [[CrossRef](#)]
31. Ying, T.; Tan, G.-X.; Ning, C.-Y.; Rong, X.-C.; Yu, Z.; Lei, Z. Bioinspired polydopamine functionalization of titanium surface for silver nanoparticles immobilization with antibacterial property. *J. Inorg. Mater.* **2014**, *29*, 1320–1326. [[CrossRef](#)]
32. Wang, R.; ho Shin, C.; Park, S.; Cui, L.; Kim, D.; Park, J.-S.; Ryu, M. Enhanced antibacterial activity of silver-coated kapok fibers through dopamine functionalization. *Water Air Soil Pollut.* **2015**, *226*, 1–9. [[CrossRef](#)]
33. Feng, X.; Jiang, L. Design and creation of superwetting/antiwetting surfaces. *Adv. Mater.* **2006**, *18*, 3063–3078. [[CrossRef](#)]
34. Yun, S.H.; Ingole, P.G.; Kim, K.H.; Choi, W.K.; Kim, J.H.; Lee, H.K. Properties and performances of polymer composite membranes correlated with monomer and polydopamine for flue gas dehydration by water vapor permeation. *Chem. Eng. J.* **2014**, *258*, 348–356. [[CrossRef](#)]
35. Bhushan, B. Bioinspired structured surfaces. *Langmuir* **2012**, *28*, 1698–1714. [[CrossRef](#)] [[PubMed](#)]
36. Cassie, A.; Baxter, S. Wettability of porous surfaces. *Trans. Faraday Soc.* **1944**, *40*, 546–551. [[CrossRef](#)]
37. Shao, L.; Wang, Z.X.; Zhang, Y.L.; Jiang, Z.X.; Liu, Y.Y. A facile strategy to enhance PVDF ultrafiltration membrane performance via self-polymerized polydopamine followed by hydrolysis of ammonium fluotitanate. *J. Membr. Sci.* **2014**, *461*, 10–21. [[CrossRef](#)]
38. Han, G.; Zhang, S.; Li, X.; Widjojo, N.; Chung, T.-S. Thin film composite forward osmosis membranes based on polydopamine modified polysulfone substrates with enhancements in both water flux and salt rejection. *Chem. Eng. Sci.* **2012**, *80*, 219–231. [[CrossRef](#)]
39. Wright, A.; Thompson, M. Hydrodynamic structure of bovine serum albumin determined by transient electric birefringence. *Biophys. J.* **1975**, *15*, 137–141. [[CrossRef](#)]
40. Dong, S.; Dong, S.; Tian, X.; Xu, Z.; Ma, D.; Cui, B.; Ren, N.; Rittmann, B.E. Role of self-assembly coated Er³⁺: YAlO₃/TiO₂ in intimate coupling of visible-light-responsive photocatalysis and biodegradation reactions. *J. Hazard. Mater.* **2016**, *302*, 386–394. [[CrossRef](#)] [[PubMed](#)]
41. Drelich, J.; Chibowski, E.; Meng, D.D.; Terpilowski, K. Hydrophilic and superhydrophilic surfaces and materials. *Soft Matter* **2011**, *7*, 9804–9828. [[CrossRef](#)]

